STM JOURNALS

Research & Reviews: Journal of Physics
ISSN: 2278-2265 (Online), ISSN: 2347-9973 (Print)
Volume 8, Issue 1
www.stmjournals.com

A Study on the Effect of Perlite Nanoclay in PVdF-co-HFP/Li-BETI Composite Eletrolytes by XRD AC Impedance and FTIR Studies

Carol Stanly Semler[1], Mohamed Tharik[1], Palaniswamy Vickraman[2], Natarajan Kirubanand[1,*]

[1]Research Scholar, Department of Physics, Gandhigram Rural Institute, Gandhigram, Dindigul, Tamil Nadu, India

[2]Professor, Department of Physics, Gandhigram Rural Institute, Gandhigram, Dindigul, Tamil Nadu, India

Abstract

In the present study, mica family of phyllosilicates, the perlite nanoclay (80–190 nm) effect as a filler in consonance with EC:DMC (1:1) v/v ratio on PVdF-co-HFP-Li-BETI matrix has been investigated by ac impedance, XRD and FT-IR vibrational spectroscopy. The ionic conductivity of the order of 10^{-7}–10^{-4} Scm^{-1} has been observed at the minimum participation of clay platelets is noted than its huge presence the non-polar phase of the PVdF has been considerably suppressed as noted XRD. The vibrational bands of characteristics PVdF crystal have gone the intensity variations very doublets with increase in clay particulates, suggestive of the metal complex formation with it, has been observed.

Keywords: *Nanoclay, filler, PVdF, composite, electrolyte, polymer.*

****Author for Correspondence*** E-mail: nkirubanand@gmail.com

INTRODUCTION

The turn 20th century and birth of 21st century have enormously bestowed the contribution and exploration of electronic gadgets such as can-camera, mobile phones, and devices for aerospace applications and so on. The demand of unprecedented evoking of utilization of rechargeable batteries with reference to energy density, realized on reviewing the battery components' physiochemical properties for lithium ion batteries i.e. cathodes, anodes and solid electrolytes. Numerous investigations on polymer electrolytes embarked a series of polymer electrolytes encompassing dry, gel and composite and nanocomposite polymer electrolytes. The utility of them as a separator cum electrolyte in lithium-ion batteries demands certain requirements as an electrolyte as well as separator. As an electrolyte, the membrane should have the conductivity in the range of 10^{-1} to 10^{-4} Scm^{-1} at room temperature, and as a separator they should have superior mechanical strength to withstand their compatibility during charging and discharging processes with reference to cathode and anode.

To achieve the requisites of the polymer electrolyte membrane, numerous host matrices PVC [1], PMMA [2–16], PEO [17], PAN [18] and so on and numerous electrolytes $LiClO_4$, $LiCF_3So_4$ [19], $LiTF_6$, $LiBF_4$, Li-imide, $LiPF_6$, LiBETI, Li-dioxelo Borate, numerous metal oxides SiO_2 [20], TiO_2 [20], ZrO_2, Al_2O_3, Metal oxides and so on and numerous plasticizers EC, PC, DEC, DMC, DOP, DEP, DES, Butyrolactone and so on, have been attempted. All the above furnished ingredients are having cost oriented, and certain stages showed the anomalous behavior such as dendrite formation (SEI phase), short circuiting, leakage of volatile solvents either in electrochemical properties and physiochemical properties.

So the cost effective ingredient, that is, nanoclay materials had been dispersed in order to have better mechanical, physical, flame retardancy and enhanced ionic conductivity and consequently achieved than the metal oxide, ceramic oxides and so on. Thus at the mid of 21st century, many academics, research

institutes and industries worldwide have attempted to fabricate the polymer nanocomposite materials based on nanoclay and as a result, the composites material with nanoclay material dispersed have emerged a new class materials with cost effective triggered accelerating research on polymer nanocomposite clay material. This insight has reflected on preparation of polymer nanocomposite electrolyte for Li-ion batteries using cost effective nanoclay materials (a minerals of layered silicates otherwise known as phyllosilicates).

MATERIALS AND METHODS

Materials

Poly(vinylidene fluoride) (PVDF) with 12 mol% of hexafluoro propylene (HFP), supplied by Solvay (solexis), France, with trade name Solef, of molecular weight 5.34×10^5 g/mol was used. The plasticizers ethylene carbonate (EC) and dimethyl carbonate (DMC) were obtained from Aldrich, USA and used as such. The perlite particle of size 80–190 nm and molecular weight 258.2 g/mol, was purchased from Nanoshel LLC, Intelligent materials Pvt. Ltd.

The solvent tetrahydrofuran (THF), HPLC grade was purchased from E. Merck, India and used without further purification. Lithium bis(perfluoroethanesulfonyl) imide (BETI) of molecular weight 387.13 g/mol was purchased from Fluka, USA and used as received. Polymer NanoClay Composite Electrolytes (PNCCEs) (membranes) were prepared as per the composition given Table 1 by solution casting technique. Figure 1 shows the structures of all the materials.

Perlite Nanoclay

Perlite clays have a 2:1 structure of primary mica minerals. Perlite contains either Al^{3+} or Mg^{2+} and Fe^{2+} as normal octahedral ions, and tetrahedral sheets in which Al^{3+} occurs as a substituted ion in place of some of the Si4+. Perlite differs from the micas in that it contains hydrated cations rather than unhydrated K^+ in the interlayer space. Layer spacing ranges from 1.0 to 1.5 nm or more. Figure 2 below displays the perlite structure and its composition.

Sample Preparation

The preparation of PNCCEs has been carried out using solution casting technique. The required quantities of polymer, filler, salt and plasticizer in wt% shown in Table 1 were mixed in a common solvent tetra hydro furan (THF). The ingredients were allowed to full dispers, and swell requires 24 h. After 24 h, the particular composition of the every solution had been sonicated for 15–30 min in order to ensure high homogeneity of solution. Immediately after the sonification, the stock solution of particular composition had been stirred and monitored at room temperature till the formation of viscous solution was obtained. The semisolid viscous solution was poured onto circular petty dishes, so as to evaporate the THF. Complete drying had taken place in about 48–78 h. The peeled off free standing films were incubated in vacuum oven at 100°C with the pressure of 10^{-5} torr. Further removed some traces of solvent. Thus the complete free standing films as prepared were kept in vacuum controlled desiccator for further characterization studies. Figure 3 shows the sample preparation technique.

Methods

Ionic conductivities of PNCCEs were studied by using HIOKI 3532-50 LCR Hi-tester in the frequency range 50 Hz–5 MHz with conductivity cell consisting of two circular stainless steel blocking electrodes (SS/PNCCEs/SS) of 1 cm^2 cross-sectional area. FTIR spectra of PNCCEs were recorded using perkinelmer/spectrum 2 spectrophotometer in the wave number range from 4000 to 400 cm^{-1} at a resolution of ±5 cm^{-1}. XRD analysis was carried out to investigate the crystalline nature of PNCCEs using a PAN-Analytical X'PertPRO powder X-ray Diffractometer Cu Kα(λ=1.54060 A°), over the range of 2θ=10–80° at 25°C temperature.

RESULT AND DISCUSSION

Ionic Conductivity Studies

PVdF-co-HFP/LiBETI/Perlite:EC:DMC Composite Electrolytes (PNCCEs) PER

The AC impedance measurement on polymer nanoclay composite electrolytes (PNCCEs) membranes has been carried out by sandwiching them in between the two stainless steel electrodes, otherwise known as blocking

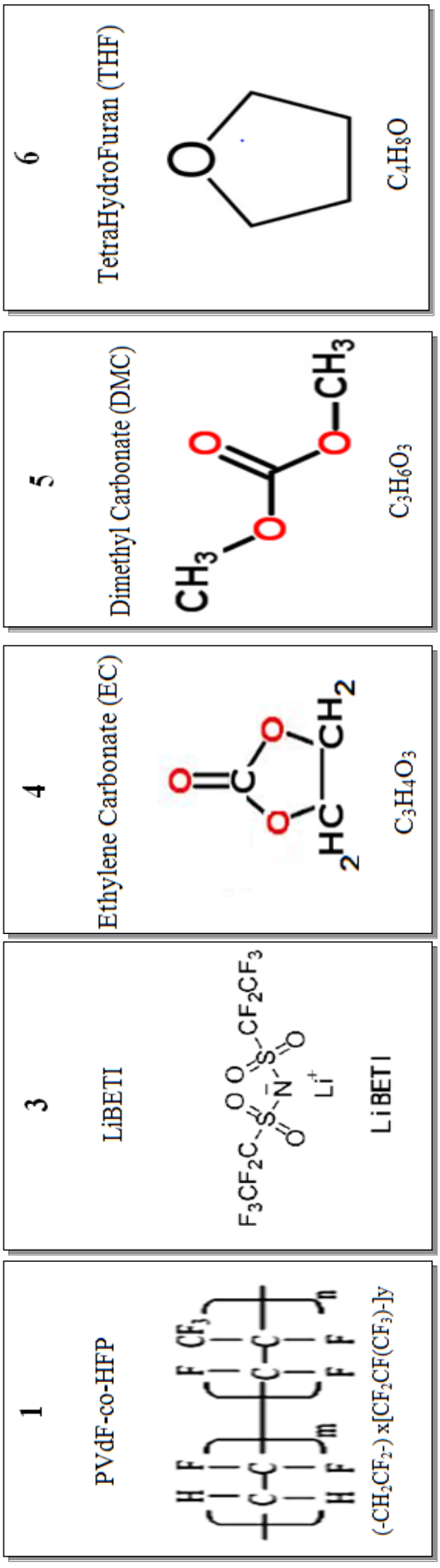

Fig. 1: *Materials Structure.*

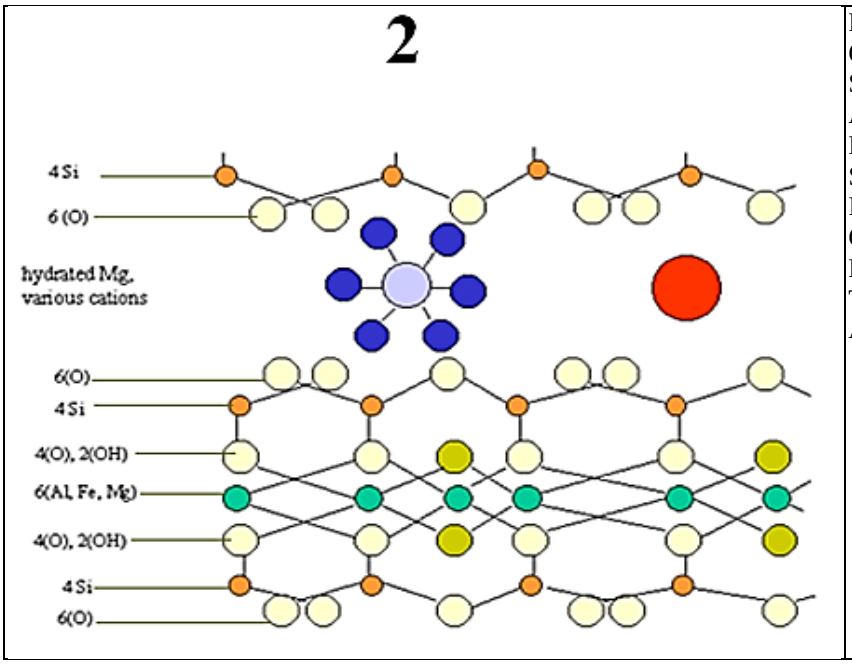

Purity	:99%
Oxygen	: 47.5 %
Silicone	: 33.8 %
Aluminum	: 7.2 %
Potassium	: 3.5 %
Sodium	: 3.4 %
Iron	: 0.6 %
Calcium	: 0.6 %
Magnesium	: 0.25 %
Traces	: 0.2 %
All Other Metal	: <0.1 %

Fig. 2: *Perlite Structure.*

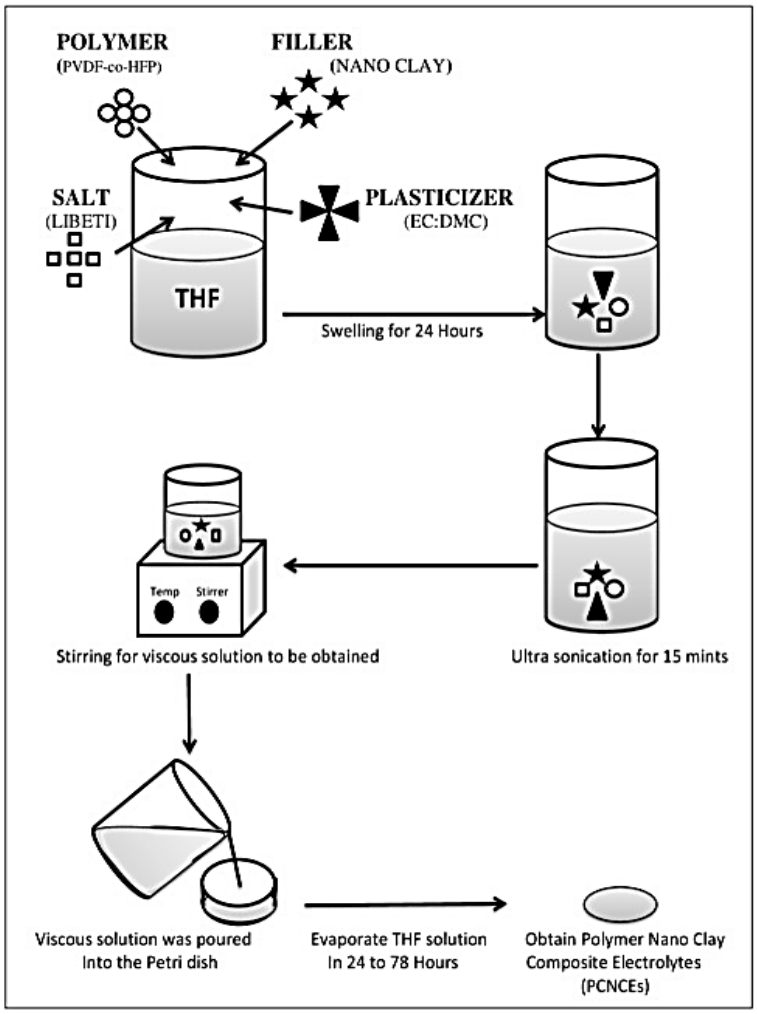

Fig. 3: *Sample Preparation Technique.*

electrodes, constitutes electrochemical cell arrangement at various frequencies ranging from 50 Hz–5 MHz. The Nyquist plot, a kind of a plot is used for evaluating AC impedance data in this dissertation.

Thus AC impedance studies begin by considering the blocking electrode setup. An AC voltage is applied to the cell and the frequency is varied. The equivalent circuit representing the AC response of the cell is shown in Figure 4. The electrodes become alternatively positively and negatively charged and the alternating field across the electrolyte causes the lithium ions to migrate back and forth in phase with the voltage. The migration of the lithium ions is represented by the resistor R_g. At the same time, the immobile polymer chains become polarized in the alternating field, just as they would if the polymer film were devoid of mobile charges and this dielectric polarization may be represented by a capacitor C_b.

$$C_b = \frac{\varepsilon\varepsilon_0 A}{l}$$

The bulk polarization and ionic migration are physically in parallel, therefore their representative components, R_b and C_b, are connected in parallel, both are in series with the electrode capacitance C_e. For a cell with electrode separation l=1 cm, and electrode area A=1 cm^2, the bulk and electrode capacitances are typically $\approx 10^{-12}$ and 10^{-6} F respectively. C_b is simply related to the dielectric constant of polymer. Since C_e is in series with the parallel combination of R_b and C_b, the equation for the total impedance is obtained simply by adding the impedance of the capacitor C_e to that of the parallel RC combination as derived.

$$Z^*_{total} = R_b\left[\frac{1}{1+(\omega R_b C_b)^2}\right] - j\left(R_b\left[\frac{\omega R_b C_b}{1+(\omega R_b C_b)^2}\right] + \frac{1}{\omega C_e}\right)$$

The complex impedance plot predicted by this equation is given in Figure 4. Because of the frequency-dependent impedance of capacitor, the full equivalent circuit of Figure 4 reduces to simpler equivalent circuits over limited frequency ranges. At the high frequencies, when the impedance of the bulk resistance and capacitance are of the same magnitude $1/\omega C_b \approx R_b$ both the bulk resistance and capacitance contribute significantly to the overall impedance, whereas the impedance of the electrode capacitance, C_e, is insignificant ($C_e \approx 10^6$ C_b). Therefore at high frequencies, the equivalent circuit reduces to a parallel R_bC_b combination which gives rise to the semicircle in the complex impedance plane. At low frequencies, $1/\omega C_b \ll R_b$ and hence C_b makes a negligible contribution to the impedance, the equivalent circuit thus reduces to a series combination of R_b and C_e appearing as a vertical spike displaced a distance R_b along the real axis. At very low frequencies, the equivalent circuit would simply be the electrode capacitance C_e only.

It is generally true that the high-frequency response yields information about the properties of the electrolyte. For example, the high-frequency semicircle yields the bulk resistance R_b and, knowing R_b and ω_{max}, the bulk capacitance, C_b, from $\omega_{max}R_bC_b=1$. The low-frequency response on the other hand carriers information on the spike, $C_e=1Z\omega$. Overall, the magnitude of all the fundamental electrical properties of the cell may be obtained from the complete impedance data. In particular, R_b is the effective DC resistance of the electrolyte; therefore simply by sandwiching a polymer electrolyte between two blocking electrodes, the DC conductivity of the electrolyte may be very easily determined [21].

The AC impedance measurements on as prepared trinery system of (PER 3) consisting of polymer perlite nanoclay and LiBETI (proportion shown in Table 1) provided the conductivity in the order of 10^{-7} Scm^{-1} which has been improved in one order of magnitude, that is, 10^{-5} Scm^{-1} while loading with EC (PER 4) is obtained. When sample 4 is further processed with DMC, it has shown the same order of the magnitude. So the plasticizing effect on the ternary component has well been understood that the plasticizer interaction of polymer is shown when PNCCEs have been examined by varying the composition dependents of filler and plasticizer. It is noted that filler free membrane (PER 6) has shown the order of the conductivity to 10^{-5} Scm^{-1}. But loading it in minimal wt% (1.5 wt%) has appreciably increased the order of the conductivity to 10^{-4} Scm^{-1} but beyond the

loading of clay in steps of 1.5 wt% increment have decreased the ionic conductivity to one order (10^{-5} Scm^{-1}) 6 wt% and two order for (PER 11). Figures 5 and 6 show AC impedance studies of PER 3–PER11.

The reason for the enhanced conductivity may be attributed to the clay platelets in minimal wt% forbids the ion-pair formation and the free anions had been arrested or trapped with metals presents in clay platelets and provides good mobility of the charge carriers which gives rise to improved conductivity. At higher loading of nanoclay, platelets the PNCCEs with filler, without filler, and increasing the filler as shown in Table 1.

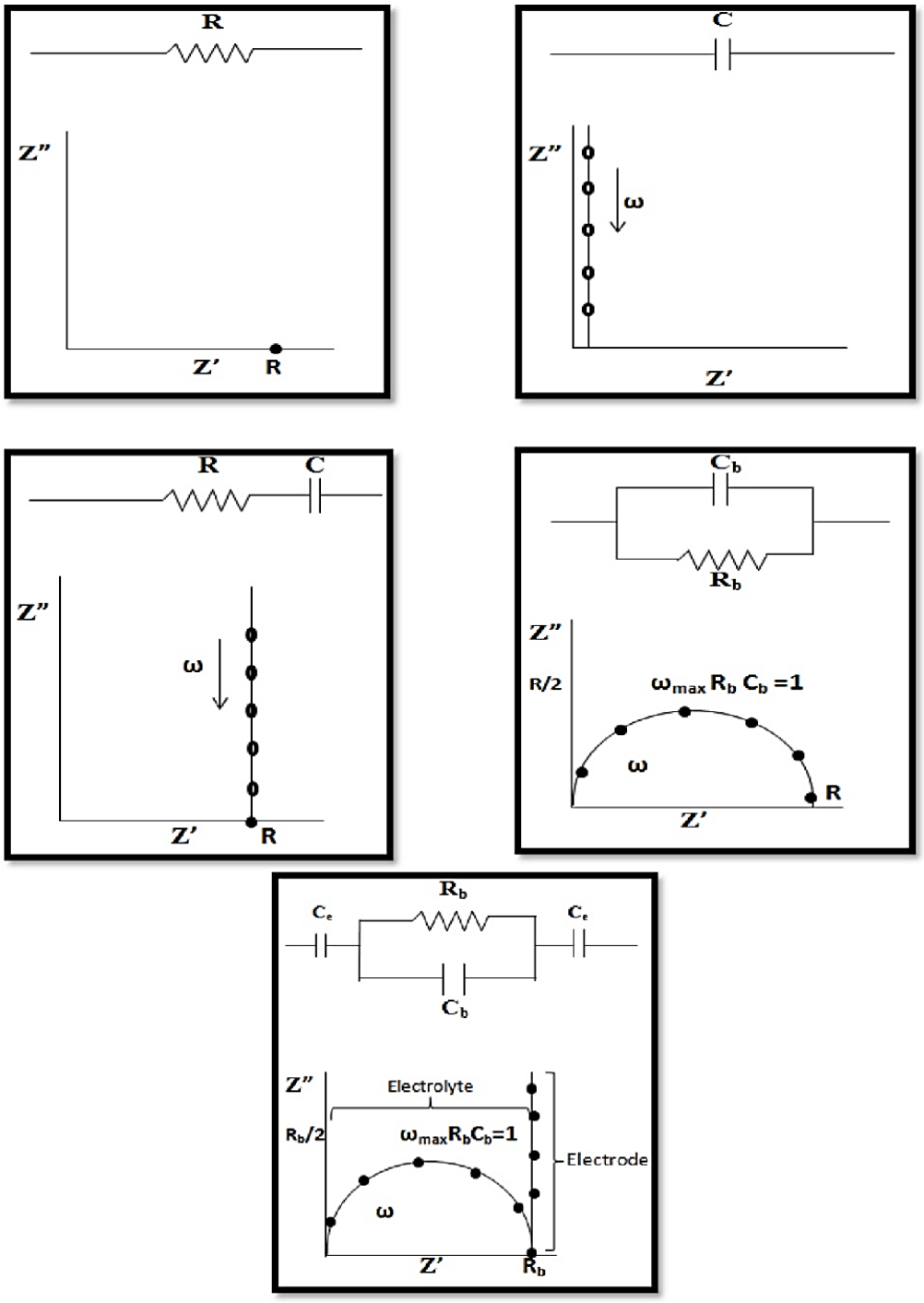

Fig. 4: *Equivalent Circuits.*

Table 1: *Composition and Ionic Conductivities of PNCCE*$_S$.

Sample Code	PVdF-co-HFP (wt%)	Perlite (wt%)	LiBETI (wt%)	EC: DMC (wt%)	Ionic Conductivity (Scm-1)
PER-1	25	0	0	0 : 0	_
PER-2	25	5	0	0 : 0	_
PER-3	25	5	5	0 : 0	9.46×10^{-7}
PER-4	25	5	5	35 : 0	1.09×10^{-5}
PER-5	25	5	5	32.5 : 32.5	4.87×10^{-5}
PER-6	25	0	5	35 : 35	5.58×10^{-5}
PER-7	25	1.5	5	34.25 : 34.25	2.62×10^{-4}
PER-8	25	3	5	33.5 : 33.5	2.42×10^{-5}
PER-9	25	4.5	5	32.75 : 32.75	1.20×10^{-5}
PER-10	25	6	5	32 : 32	2.90×10^{-5}
PER-11	25	7.5	5	31.25 : 31.25	5.23×10^{-6}

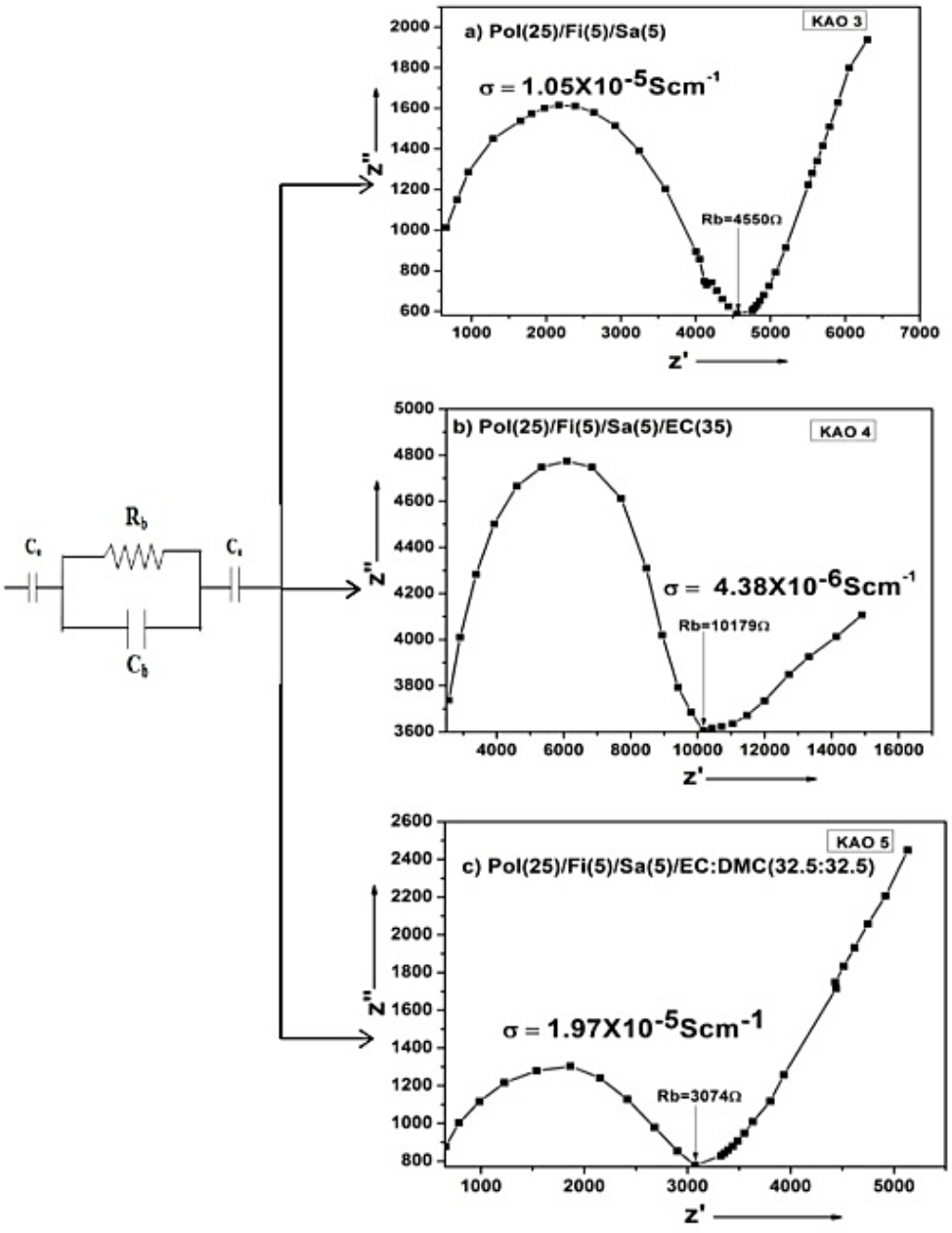

Fig. 5: *A.C. Impedance Studies of (a) PER 3, (b) PER 4, (c) PER 5.*

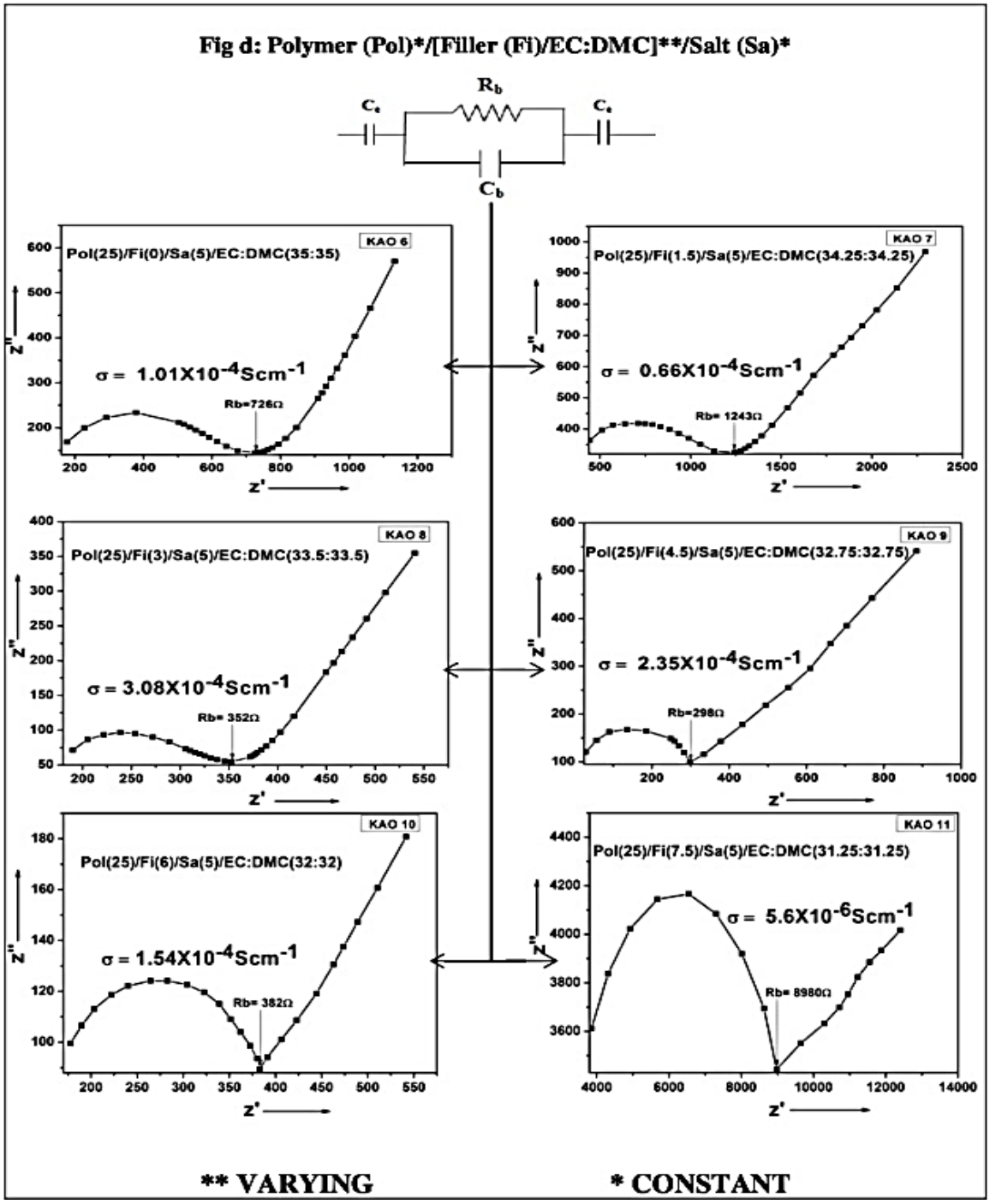

Fig. 6: *A.C. Impedance Studies of PER 6, PER 7, PER 8, PER 9, PER 10 and PER 11.*

In this study, different clays in nanosize less than or equal to 82–100 nm have been dispersed as a solid plasticizers to dissociate into lithium (Li^+/cations) and Li^- anions gives rise to the number of charge carriers and also facilitating their mobility through the process called intercalation and exfoliation. In the intercalation process, the gallery spacing between the layered silicates due to the protrusion of chain molecules of PVdF widened. This widening and the interaction between the polar group of the polymer and the charge effects of the surface clays provides pathway for the lithium (Li^+) cations for gaining momentum which provides the mobility, and as a result, ionic conductivity variations are observed on the other hand in the exfoliation process due to the increase in

the concentration of clay platelets. In the present study, 3, 4.5, 6 and 7.5 wt%, their distorted intercalation or exfoliation takes place, wherein the PVdF molecules have coiled down the layered sheets and distorting them in such a way that the Li^+ cations thus generated in our case, 1.5 wt% have been masked or constricted Li+ cation movement resulting in decrementing ionic conductivity.. Figure 7 presents the schematic representation of polymer intercalation in clay platelets.

Thus the intercalation and exfoliation are said to be phenomena of interaction between layered silicates and the polar polymers PVdF interactions between them have showed the polymers, nanocomposite clay electrolytes change in their crystallinity and amorphousity. The crystallinity and amorphousity of the membranes have been subjected to XRD studies, by varying the compositional dependence of plasticizer and clay concentration. In general, plasticizer, when it is added with the polymer it gives rise to the flexibility to the polymer chains enabling Li^+ cations transit by hopping mechanism through the end points of chain segments. In our case, the plasticizers are used to do the process of flexing the polymer host as well as dissoluting Li^+ salts for generating charge carriers for conductivity and converting certain crystallite phases of PVdF into amorphous phase. In this study, the plasticizer rich phase with clay poor phase have not profusely changed the intensity of their characteristic phases of PVdF and the filler rich phase with poor plasticizer phase have also not contributed much in the change of phase of PVdF.

XRD Studies

The XRD study on pristine PVdF-co-HFP is labeled as (PER 1). The characteristic peaks observed at 17.8°(110) [22], 18.24°(020) [23], 19.82°(110) [24] correspond to VdF crystals of α-phase. These α phase crystallites have all disappeared rather no trace of them while adding perlite is noted in 10–20° range, however their performance have well been defined in 20–40°. Table 2 reveals that α-phase crystals are located at in the chain segment is noted. When nanoclay is added to this sample, no trace of α-phase crystallites in 10–20° and repeatability of them 20–40° as similar to (PER 2) are noted. When EC is added (PER 4), certain characteristic peaks in 10–20° disappeared. Suppressed, except 19.97° in 10–20° and 38° in 20–40°, α crystal plane is absent [25]. This, similarly in crystalline planes is noted while adding DMC to the matrix. From this above observation, it is evident that the plasticizing effect could be seen in 20–40°.

The crystalline and amorphous phase presence has been examined by varying filler/plasticizer wt%. Of all the samples starting from filler free membrane to 6 wt% of it have shown that increase in amorphous phase resulted in enhanced conductivity as noted support AC impedance measurements (Figures 8 and 9).

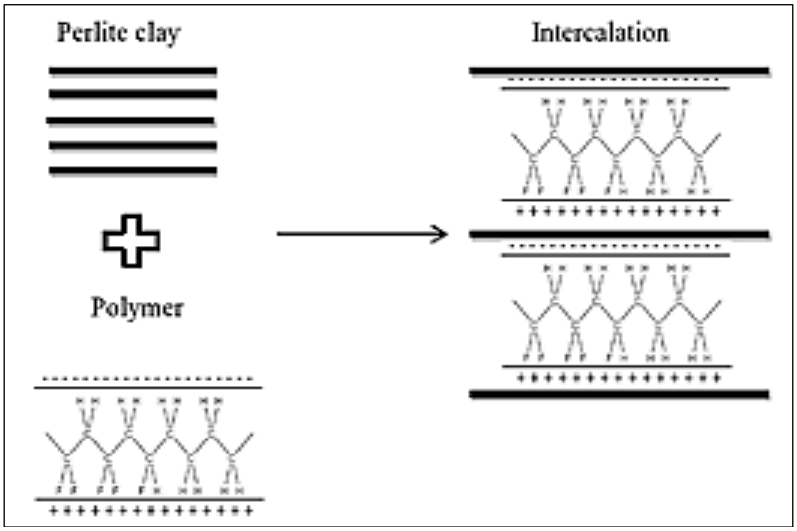

Fig. 7: *Schematic Representation of Polymer Intercalation in Clay Platelets.*

***Table 2**: Composition and XRD Peak Appearance of PNCCE$_S$.*

Sample Code	PVdF-co-HFP (wt%)	Perlite (wt%)	LiBETI (wt%)	EC : DMC (wt%)	XRD 2Θ (°)	
					10–20°	20–40°
PER-1	25	0	0	0 : 0	17.80(110–α) 18.24(020–α) 19.82(110–α)	26.01(021–α)
PER-2	25	5	0	0 : 0	19.89(110–α)	26.64(021α+γ) 39.34
PER-3	25	5	5	0 : 0		20.15 30.13 39.61
PER-4	25	5	5	35 : 0		20.10
PER-5	25	5	5	32.5 : 32.5		20.34(110/200β)
PER-6	25	0	5	35 : 35		20.21(110α+γ)
PER-7	25	1.5	5	34.25 : 34.25		19.87(110–α)
PER-8	25	3	5	33.5 : 33.5	10.17	20.26(110α+γ)
PER-9	25	4.5	5	32.75 : 32.75		20.28(110α+γ)
PER-10	25	6	5	32 : 32	19.88(110–α)	
PER-11	25	7.5	5	31.25 : 31.25		

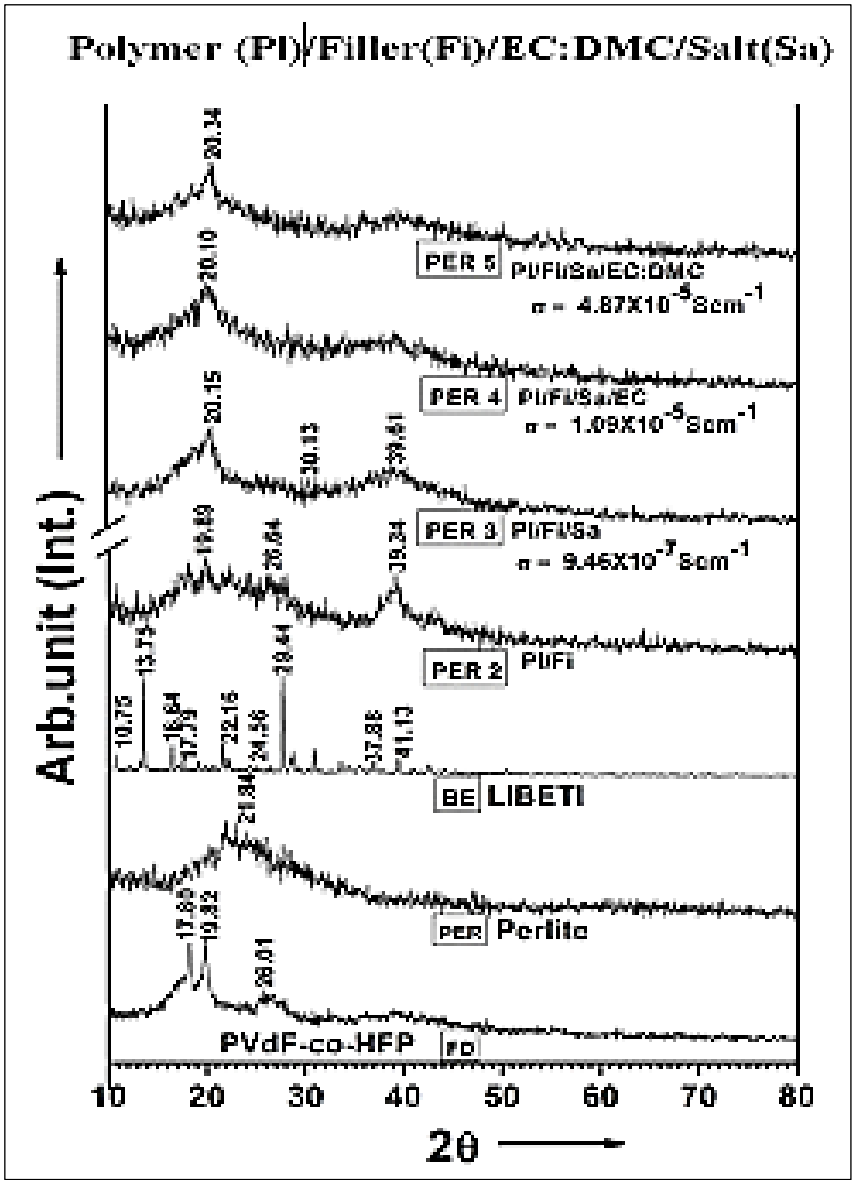

***Fig. 8:** XRD Diffractogram of FD, PER, BE, PER 2 and PNCCEs (PER 3, PER 4, PER 5).*

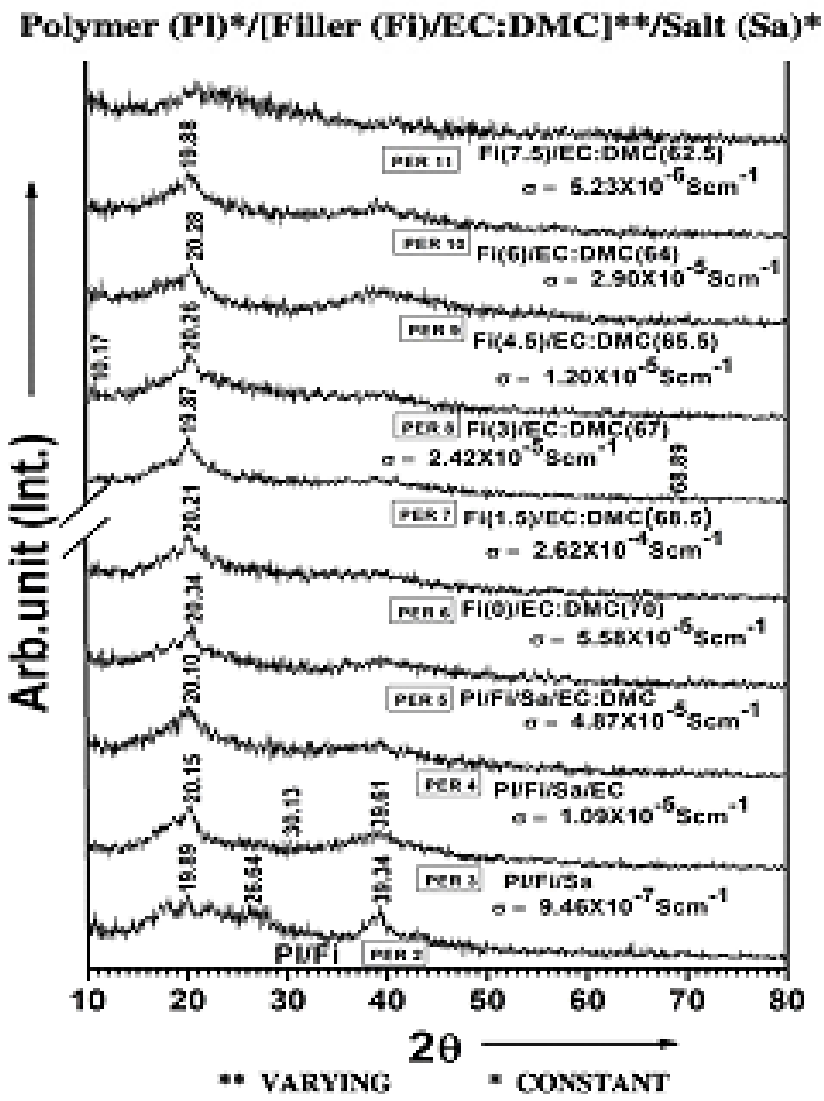

***Fig. 9**: XRD Diffractogram of PNCCEs PER 2, PER 3, PER 4, PER 5, PER 6,PER 7, PER 8, PER 9, PER 10 and PER 11.*

FT-IR Studies

FT-IR vibrational spectroscopy studies on PNCCEs have been carried out to elucidate the complexation of various constituents at the molecular level in the IR region of 400–4000 cm^{-1} wave number. All the pristine natures of constituents of PNCCEs have been recorded. As a first step, the pristine PVdF-co-HFP has shown the characteristics vibrational bands such as 488 cm^{-1} (sharp), 513 cm^{-1}(a small kink like appearance not as a band at all) and a medium sharp peak at 610 cm^{-1}, then 759 cm^{-1}(a distinct singlet, medium)/874 cm^{-1}(strong singlet, sharp), and in 1000–1200 cm^{-1} region, the doublet one with a very minimum intensity 1068 cm^{-1} co-folding with very sharp 1159 and 1396 cm^{-1} corresponds to the α-phase of VdF crystals and C-F grouping (stretching, wagging on) amenable to the vibrational modes reported elsewhere [26, 27].

When perlite is dispersoid and, as prepared polymer clay binary system showed the variation in intensities and with slight shifts in vibrational bands could well be noted, i.e., a 488 cm^{-1} drastically reduced in intensity, the 513 cm^{-1} kink like appearance well formed, the medium sharp 610 cm^{-1} drastic reduction and the reduction in intensities of 1068/1179 cm^{-1} doublet and 1396 cm^{-1} intensity detection have all corresponded to intercalation of nanoclay platelets with polymer, is very well noted. The

subsequent addition of LiBETI and as prepared trinary have shown that intensity variations in the characteristics vibrational band as that of the binary system.

When EC is added to trinary system to process the flexibility to the chain segments of the host matrix as well as dissoluting lithium salts, as a result the 488 cm^{-1} sharp band appeared at 430 cm^{-1} towards the lower wave number region (broadened), the well grown 610 cm^{-1} peak in trinary system is highly suppressed and emergence of two short peaks appeared. As far as the 1068/1170 cm^{-1} doublet is concerned, the intensity of them has grown with the symmetry and the new appearance of C=O carbonyl band as noted. Thus the role of EC with the host matrix has been understood. When DMC is added and as prepared as again shows the intensity variations of the vibrational bands, particularly the well grown 1072/1186 cm^{-1} and the symmetric and asymmetric stretching modes of C=O, thus starting up with mono system of polymer host that binary, trinary, tetra, and penta system have highlighted the degree of interaction of the polar group of the polymer C-F and the conformational phases of host.

When the PNCCEs have been examined by varying filler plasticizer weight ratio while keeping polymer and salt content as constant, some phenomenological observations have been noted that very minimal nanoclay particulate has enormously improved the intensity contours of the doublets 1072/1186 cm^{-1} with shifts 1069/1158 cm^{-1} and the carbonyl band symmetric and asymmetric capping's has been very appreciably enhanced suggesting that the plasticizer has well been interacted with the very less minimal dispersoid 1.5 wt%; but the increase the loading of clay platelets till to 7.5 from 3 wt% has profusely reduced the intensity detection with the consistency, has shown that the nanoclay concentration has an important role regarding the complexation of the constituents of PNCCEs (Table 3 and Figures 10 and 11).

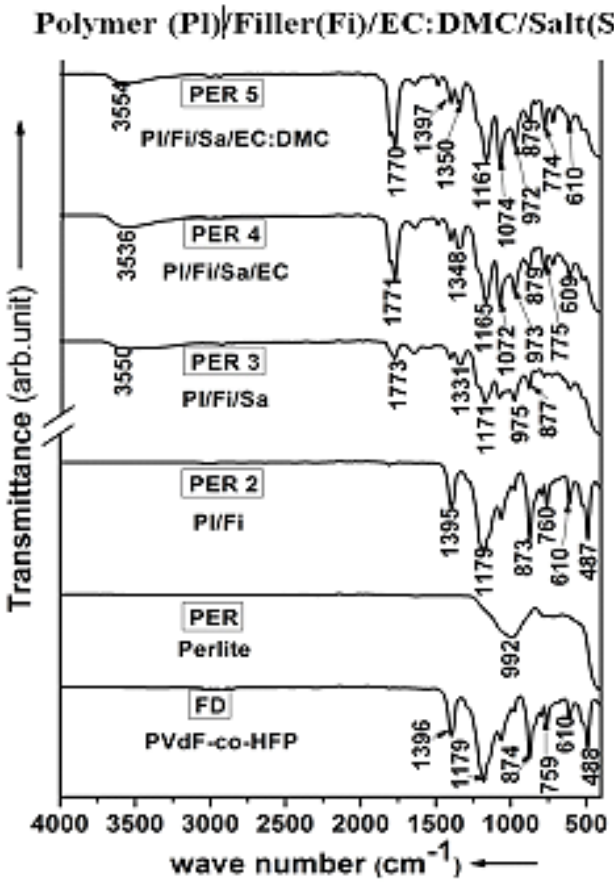

Fig. 10*: FT-IR Studies of FD, PER, PER 2, and PNCCEs (PER 3, PER 4, PER 5).*

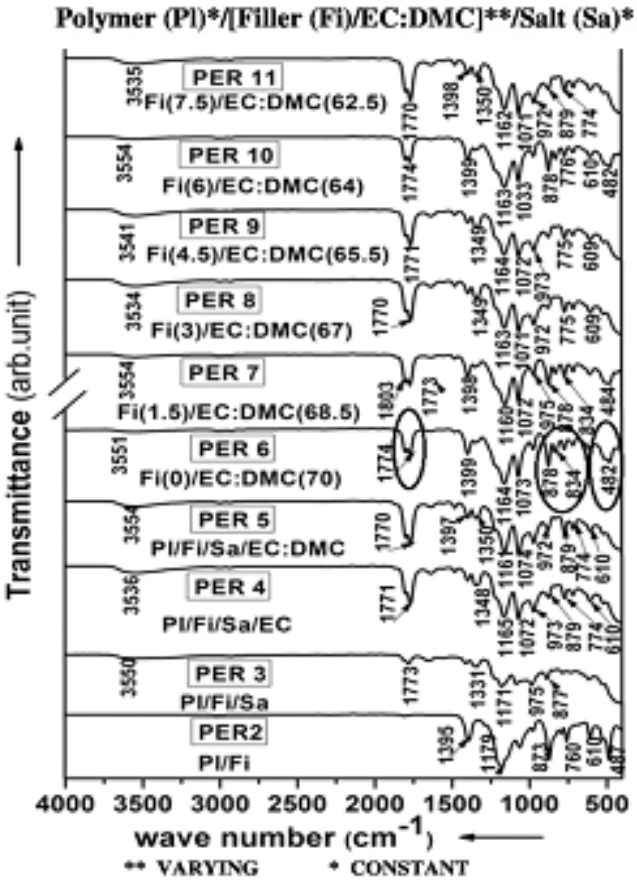

Fig. 11: *FT-IR Studies of PNCCEs PER 2, PER 3, PER 4, PER 5, PER 6, PER 7, PER 8, PER 9, PER 10 and PER 11.*

Table 3: *Vibrational Bands of PNCCEs.*

Wave Number (cm^{-1})	PER 1	PER 2	PER 3	PER 4	PER 5	PER 6	PER 7	PER 8	PER 9	PER 10	PER 11
	Medal Oxide Region										
400	438	487				482	484			482	
500											
600	610	610		610	610			609	609	610	
	Finger Print Region										
700	759	760		774	774			775	775	776	774
800	874	873	877	879	879	834 878	834 878			878	879
900			975	973	972		975	972	973		972
1000	1062			1072	1074	1073	1072	1071	1072	1033	1071
1100	1179	1179	1171	1165	1161	1164	1160	1163	1164	1163	1162
1200											
1300	1396	1395	1331	1348	1350 1397	1399	1398	1349	1349	1399	1350 1398
1400											
1500											
	Functional Group Region										
C=O			1773	1771	1770	1774	1773	1770	1771	1774	1770

REFERENCES

1. Ahn JH, Wang GX, Liu HK, *et al.* Nanoparticle-Dispersed PEO Polymer Electrolytes for Li Batteries. *J Power Sources*. 2003; 119–121: 422–426p.
2. Bohnke O, Frand G, Rezrazi M, *et al.* Fast Ion Transport in New Lithium Electrolytes Gelled with PMMA-Influence of Polymer Concentration. *Solid State Ionics*. 1993; 66(1–2): 97–104p.
3. Bohnke O, Frand G, Rezrazi M, *et al.* Fast Ion Transport in New Lithium Electrolytes Gelled with PMMA. 1. Influence of Polymer Concentration. *Solid State Ionics*. 1993(b); 66(1–2): 105–112p.
4. Bohnke O, Rousselot C, Gillet C, *et al.* Gel Electrolyte for Solid-State Electrochromic Cell. *J Electrochem Soc.* 1992; 139(7): 1862–65p.
5. Appetecchi G, Croce F, Scrosati B. Kinetics and Stability of the Lithium Electrode in Poly(Methylmethacrylate)-Based Gel Electrolytes. *Electrochim Acta*. 1995; 40(8): 991–997p.
6. Ostrovskii D, Torell L, Appetecchi G, *et al.* An Electrochemical and Raman Spectroscopical Study of Gel Polymer Electrolytes for Lithium Batteries. *Solid State Ion*. 1998; 106(1–2): 19–24p.
7. Osaka T, Momma T, Ito H, *et al.* Performances of Lithium/Gel Electrolyte/Polypyrrole Secondary Batteries. *J Power Sources*. 1997; 68(2): 392–396p.
8. Sekhon S, Pradeep S, Agnihotry S, *et al.*, editors. Conductivity and Viscosity of Liquid and Gel Electrolytes Based on LiClO4, LiN(CF3SO2)2 and PMMA, Solid State Ionics: Science and Technology, World Scientific, 1998; 217p.
9. Sekhon S, Deepa M, Agnihotry S. Solvent Effect on Gel Electrolytes Containing Lithium Salts. *Solid State Ion*. 2000; 136–137: 1189–1192p.
10. Kim C, Lee K, Kim W, *et al.* Ion Conductivities and Interfacial Characteristics of the Plasticized Polymer Electrolytes Based on Poly(Methyl Methacrylate-co-Li Maleate). *J Power Sources*. 2001; 94(2): 163–168p.
11. Svanberg C, Adebahr J, Ericson H, *et al.* Diffusive and Segmental Dynamics in Polymer Gel Electrolytes. *J Chem Phys.* 1999; 111(24): 11216p.
12. Svanberg C, Adebahr J, Bergman R, *et al.* Polymer Concentration Dependence of the Dynamics in Gel Electrolytes. *Solid State Ion*. 2000; 136–137: 1147–1152p.
13. Svanberg C, Bergman R, Borjesson L, *et al.* Diffusion of Solvent/Salt and Segmental Relaxation in Polymer Gel Electrolytes. *Electrochim Acta*. 2001; 46(10): 1447–1451p.
14. Ostrovskii D, Brodin A, Torell L, *et al.* Molecular and Ionic Interactions in Poly(Acrylonitrile)- and Poly(Methylmetacrylate)-Based Gel Electrolytes. *J Chem Phys.* 1998; 109(17): 7618p.
15. Deepa M, Sharma N, Agnihotry A. FTIR Investigations on Ion–Ion Interactions in Liquid and Gel Polymeric Electrolytes: LiCF3SO3-PC-PMMA. *J Mater Sci*. 2002; 37(9): 1759–1765p.
16. Raghavan P, Manuel J, Zhao X, *et al.* Preparation and Electrochemical Characterization of Gel Polymer Electrolyte Based on Electrospun Polyacrylonitrile Nonwoven Membranes for Lithium Batteries. *J Power Sources*. 2011; 196(16): 6742–49p.
17. Raghavan P, Zhao X, Shin C, *et al.* Preparation and Electrochemical Characterization of Polymer Electrolytes Based on Electrospun Poly(Vinylidenefluoride-co-Hexafluoropropylene)/Polyacrylonitrile Blend/Composite Membranes, for Lithium Batteries. *J Power Sources*. 2010; 195(18): 6088–6094p.
18. Abbrent S, Plestil J, Hlavata D, *et al.* Crystallinity and Morphology of PVdF–HFP Based Gel Electrolytes. *Polymer*. 2001; 42(4): 1407p.
19. Ashrafi R, Sahu DK, Kesharwani P, *et al.* Ag+-Ion Conducting Nano-Composite Polymer Electrolytes (NCPEs): Synthesis, Characterization and All-Solid-Battery Studies. *J Non-Cryst Solids*. 2014; 391: 91–95p.
20. Verma ML, Minakshi M, Singh NK. Synthesis and Characterization of Solid Polymer Electrolyte Based on Activated Carbon for Solid State Capacitor.

Electrochim Acta. 2014; 137: 497–503p.
21. MacCallum JR, Vincent CA. *Polymer Electrolytes Reviews*. New York: Elsevier; 1987; 248–254p.
22. Priya L, Jog JP. Poly(Vinylidene Fluoride)/Clay Nanocomposites Prepared byMelt Intercalation: Crystallization and Dynamic Mechanical Behavior Studies. *J Polym Sci Part B: Polym Phys*. 2002; 40(15): 1682–1689p.
23. Zhaohui Li, Guangyao Su, Xiayu Wang, *et al*. Micro-Porous P(VDF-HFP)-Based Polymer Electrolyte Filled with Al2O3 Nanoparticles. *Solid State Ion*. 2005; 176(23): 1903–1908p.
24. Satapathy S, Santosh Pawar, Gupta PK, *et al*. Effect of Annealing on Phase Transition in Poly(Vinylidene Fluoride Films Prepared Using Polar Solvent. *Bull Mater Sci*. Jul 2011; 34(4): 727–733p.
25. Kwang Man Kim, Nam-Gyu Park, Kwang Sun Ryu, *et al*. Characteristics of PVdF-HFP/TiO2 Composite Membrane Electrolyte Prepared by Phase Inversion and Conventional Casting Methods. *Electrochim Acta*. 2006; 51(26): 5636–5644p.
26. Silversatain RM, Webster FX. *Spectroscopic Identification of Organic Compounds*. (Chapter 3). 6th Edn. New York, USA: John Wiley and sons; 1997.
27. Pavia DL, Lampman G, Mand Kriz GS. *Introduction to Spectroscopy*. (Chapter 1). USA: Harcourt College Publication; 2001.

Cite this Article
Carol Stanly Semler, Mohamed Tharik, Palaniswamy Vickraman, Natarajan Kirubanand. A Study on the Effect of Perlite Nanoclay in PVdF-co-HFP/Li-BETI Composite Eletrolytes by XRD AC Impedance and FTIR Studies. *Research & Reviews: Journal of Physics*. 2019; 8(1): 58–72p.